10^{-4} times smaller than F^{0c} [Eq. (B1)]. The remaining integral in Eq. (B4) is even smaller than the term in Eq. (B5); hence we see that strong-collisions effects in the correlation term are negligible compared with their effects in the ideal-gas term.

The strong-collision cutoff may be included by subtracting $(F^{0c}-F^{0})$ from the F given by Eq. (A29). This is equivalent to subtracting

$$G_{sc}(\Delta\omega)=\int_0^\infty \exp(is\hbar\Delta\omega/kT)[(s^2+is)^{-1/2} - (\lambda/2x_0)\,\mathrm{erf}(\sqrt{\pi}x_0/\lambda(s^2+is)^{1/2})]ds \quad \text{(B6)}$$

from the G integral given by Eq. (A38).

PHYSICAL REVIEW VOLUME 166, NUMBER 1 5 FEBRUARY 1968

Quasisteady State in the Stimulated Brillouin Scattering of Liquids

M. MAIER
Physik-Department der Technischen Hochschule, München, Germany
(Received 3 August 1967)

Measurements of stimulated Brillouin scattering in CS_2, ethyl ether, and n-hexane with high time resolution (0.3 nsec) reveal a quasistationary state for most of the laser pulse. Conversion efficiencies between 70 and 90% were obtained. The linear relationship between Brillouin power and laser power, and the dependence of the conversion efficiency on the cell length, are in agreement with a stationary theory of stimulated Brillouin scattering. The steady-state gain factors were determined for three liquids and compared with values calculated from hypersonic data. The agreement between the theoretical and experimental gain factors is satisfactory.

I. INTRODUCTION

SINCE the first observation of stimulated Brillouin scattering (SBS) a considerable number of experimental[1–6] and theoretical[7–9] papers have appeared. Quantitative comparisons between experiments and existing theories were made very recently. Brewer[2] reported on measurements of stimulated Brillouin scattering in n-hexane and explained his data with the transient theory of Kroll.[9] Walder and Tang[3] measured the stimulated Brillouin emission in the same liquid as a function of the incident laser intensity in the region where the Brillouin power rises exponentially. They found their results in good agreement with the results of a steady-state theory[8]. Pine[4] investigated the SBS in a transverse resonator and correlated the threshold power and the peak output power of stimulated Brillouin scattering with the photoelastic parameters. Hagenlocker *et al.*[5] have compared measured gain factors for stimulated Brillouin scattering with gain factors which were calculated from a nonstationary theory; the agreement was found to be good in various substances. In all these previous measurements the laser and Brillouin intensity were integrated over the pulse time and over the cross section of the laser beam.

In this paper measurements of stimulated Brillouin scattering with high time resolution (0.3 nsec) are described. This method[6] has the advantage that a more direct comparison between theory and experiment is possible.

We have investigated the stimulated Brillouin scattering in CS_2, ethyl ether, and n-hexane. In these liquids high conversion efficiencies and a quasisteady state were observed. We wish to use the term "quasisteady state" to indicate that we are dealing with short laser pulses and not with cw light sources. A stationary theory which includes the strong attenuation of the laser beam by the Brillouin light is successfully applied to the experimental results. Furthermore, the dependence of the stimulated Brillouin power on the distance from the entrance window was investigated. These measurements were found to provide a new method to determine experimentally the steady-state gain factors for the three liquids. These gain factors were in reasonable agreement with the values calculated from the hypersonic data of the substances.

[1] R. Y. Chiao, C. H. Townes, and B. P. Stoicheff, Phys. Rev. Letters **12**, 592 (1964); E. Garmire and C. H. Townes, Appl. Phys. Letters **5**, 137 (1964); R. G. Brewer, *ibid.* **5**, 127 (1964); **9**, 51 (1966); R. G. Brewer and K. E. Rieckhoff, Phys. Rev. Letters **13**, 334 (1964); C. R. Guiliano, Appl. Phys. Letters **7**, 279 (1965); D. A. Jennings and H. Takuma, *ibid.* **5**, 241 (1964); R. N. Keeler, O. H. Bloom, and A. C. Mitchell, Phys. Rev. Letters **17**, 852 (1966); M. Maier, W. Rother, and W. Kaiser, Phys. Letters **23**, 83 (1966).
[2] R. G. Brewer, Phys. Rev. **140**, A800 (1965).
[3] J. Walder and C. L. Tang, Phys. Rev. **155**, 318 (1967).
[4] A. S. Pine, Phys. Rev. **149**, 113 (1966).
[5] E. E. Hagenlocker, R. W. Minck, and W. G. Rado, Phys. Rev. **154**, 226 (1967).
[6] M. Maier, W. Rother, and W. Kaiser, Appl. Phys. Letters **10**, 80 (1967).
[7] R. Y. Chiao, E. Garmire, and C. H. Townes, in *Proceedings of the Enrico Fermi International School of Physics* (Academic Press Inc., New York, 1964), Course XXXI, 1963; A. Yariv, J. Quant. Electron. **1**, 41 (1965); Y. R. Shen and N. Bloembergen, Phys. Rev. **137**, A1786 (1965); K. Grob, Z. Physik **201**, 59 (1967).
[8] C. L. Tang, J. Appl. Phys. **37**, 2945 (1966).
[9] N. M. Kroll, J. Appl. Phys. **36**, 34 (1965); D. L. Bobroff, *ibid.* **36**, 1760 (1965).

In Sec. II the steady-state theory of stimulated Brillouin scattering[8] which includes the attenuation of the laser beam is reviewed. For a comparison of the theory with the experimental data an expression of the Brillouin power is derived for an incoming laser beam with Gaussian intensity distribution over the cross section. Section III describes the experimental system. The results on the quasistationary state of the SBS, the dependence of the Brillouin power on the distance from the entrance window, and the steady-state gain factors follow in Sec. IV. The experimental results are compared with theory in Sec. V.

II. THEORY

It will be shown in the experimental part of this paper that in a number of liquids stimulated Brillouin emission occurs in a quasisteady state. For this reason we restrict ourselves to a discussion of the steady-state theory[7,8] of SBS. In the liquids investigated the acoustic phonons are heavily damped and the attenuation length is much shorter than the interaction region and the distance over which the intensities of the laser and Stokes waves change appreciably. It was shown by Tang[8] that in this case SBS can be described by two coupled first-order nonlinear rate equations for the photon flux densities of the laser (N_L) and the Stokes light (N_B).

$$\partial N_B(z)/\partial z = -g' N_L(z) N_B(z), \tag{1}$$

$$\partial N_L(z)/\partial z = -g' N_L(z) N_B(z). \tag{2}$$

The laser light propagates in the $+z$ direction, the Stokes light in the $-z$ direction. g' is the gain factor. The photon flux densities N are connected with the amplitudes E of the laser or Stokes wave.

$$\begin{aligned} N_L(z) &= (cn_L/8\pi\hbar\omega_L)\,|E_L(z)|^2; \\ N_B(z) &= (cn_B/8\pi\hbar\omega_B)\,|E_B(z)|^2. \end{aligned} \tag{3}$$

Both waves were assumed to be plane waves of the form $E_L' = \frac{1}{2}(E_L e^{i(k_L z-\omega_L t)} + \text{c.c.})$ and

$$E_B' = \tfrac{1}{2}(E_B e^{i(-k_B z-\omega_B t)} + \text{c.c.}).$$

c is the velocity of light, n the index of refraction, and ω_L the frequency of the laser light. Equations (1) and (2) are also valid for intensities I, since $\omega_L \simeq \omega_B$. Taking $I_L = N_L\hbar\omega_L$ and $I_B = N_B\hbar\omega_B$, we get

$$\partial I_B/\partial z = -gI_L(z)I_B(z), \tag{4}$$

$$\partial I_L/\partial z = -gI_L(z)I_B(z). \tag{5}$$

The gain factor g is given by

$$g = k_L^2\gamma^2/2\pi c n^3 \rho v \delta\nu. \tag{6}$$

γ is the electrostrictive coupling parameter, ρ the density, v and $\delta\nu$ the velocity and the linewidth of the acoustic phonons, respectively.

The solutions of (4) and (5) are:

$$\frac{I_B(z)}{I_B(0)} = \frac{1-I_B(0)/I_L(0)}{\exp\{[1-I_B(0)/I_L(0)]gI_L(0)z\} - I_B(0)/I_L(0)} \tag{7}$$

and

$$I_B(0) = I_L(0) - I_L(z) + I_B(z). \tag{8}$$

$I_L(0)$ and $I_B(0)$ are the laser and the Brillouin intensity at the entrance window, respectively.

The assumption of infinite monochromatic plane waves is never realized experimentally. We have a certain frequency spread of the laser and Brillouin line and a finite beam diameter with a definite intensity distribution over the cross section. Assuming solutions (7) and (8) to be also valid for this case, we can calculate the total power of the Brillouin emission P_B. These calculations will be compared with power data obtained directly from our experiments. The intensity distribution of our laser beam was investigated experimentally and found to be well approximated by a Gaussian function, i.e., the intensity $I_L(0)$ at the entrance window of the cell ($z=0$) is connected with the radial coordinate r by the equation: $I_L(0) = I_0 \exp[-(r/r_0)^2]$, where r_0 is the beam radius.

For a comparison with our experimental results we wish to analyse the following two items:

(1) The Brillouin power at the entrance window $P_B(0)$

(2) The dependence of the Brillouin power $P_B(z)$ on the distance z from the entrance window.

To (1) we introduce the conversion efficiency of laser light in Brillouin light by $K = I_B(0)/I_L(0)$. For high gain in a cell of length ℓ, i.e., for $\exp\{[1-K]gI_L(0)\ell\} \gg K$, Eq. (7) can be rewritten in the form

$$\begin{aligned} &(1-K)gI_L(0)\ell \\ &\quad = \ln[(1-K)K] - \ln[I_B(\ell)/I_L(0)] \equiv G. \end{aligned} \tag{9}$$

For given values of $I_L(0)$, ℓ, g, and $I_B(\ell)$,[10] Equation (9) can be used to calculate the conversion efficiency K. The calculation of K shows that the right-hand side of Eq. (9) is approximately constant for values of $I_L(0)$, ℓ and g which occur in our experiments (e.g., $10 < I_L(0) < 10^3$ MW/cm^2, $5 < \ell < 50$ cm and $0.01 < g < 0.10$ cm/MW).

For a definite value of $I_B(\ell)$ we obtain

$$(1-K)gI_L(0)\ell = G \simeq \text{const.} \tag{10}$$

Equation (10) can be solved for the Brillouin intensity at the entrance window

$$I_B(0) = I_L(0) - G/g\ell. \tag{11}$$

A comparison with an exact solution of Eq. (9) was made for the range of experimental interest defined

[10] Numerical values of $I_B(\ell)$ are given in Sec. V, (3).

above. It turned out that Eq. (11) is a good approximation for laser intensities $I_L(0) > G/g\ell$.

In our experiments the laser and Brillouin intensity change slowly within a radial distance large compared to the wavelength. In addition the influence of variations of $I_B(\ell)$ over the cross section of the beam on the value of G is very small. We can use, therefore, Eq. (11) to calculate the intensity distribution of the Brillouin light over the cross section for a given intensity distribution of the laser light. Figure 1 shows a schematic intensity distribution of the Brillouin light I_B for a given Gaussian intensity distribution of the laser light I_L and for a definite value of $G/g\ell$. Outside the range of validity of Eq. (11), i.e., for $I_L(0) < G/g\ell$ we assume $I_B(0) = 0$. An exact solution of Eq. (9) shows that this assumption is a good approximation in the experimental range of interest. We integrate Eq. (11) over the cross section of the Brillouin beam and get the dependence of the Brillouin power on the laser power at the entrance window ($z = 0$).

$$P_B(0) = P_L(0) - (GF_0/g\ell)\{1 + \ln I_0 g\ell/G\}. \quad (12)$$

Here we have used the relations

$$I_L(0) = I_0 \exp[-(r/r_0)^2] \quad (13)$$

and

$$P_L(0) = r_0^2 \pi I_0 = F_0 I_0.$$

The curly bracket in Eq. (12) originates from the upper limit of integration which is defined by $I_B(0) = 0$ or [from Eq. (11)] by $I_L(0) = G/g\ell$. The proportionality between Brillouin power and laser power and the length dependence of the Brillouin power predicted by Eq. (12) will be shown to agree quite well with the experimental observations.

To (2) in order to calculate the dependence of the Brillouin power on z, we introduce Eq. (11) into Eq. (7) and get

$$I_B(z) = \frac{G}{g\ell} \frac{I_L(0) - G/g\ell}{\{[\exp(Gz/l)] - 1\} I_L(0) + G/g\ell}. \quad (14)$$

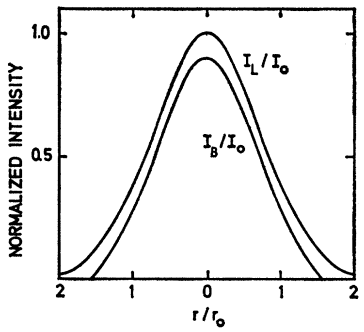

FIG. 1. Schematic intensity distribution of the normalized Brillouin light I_B/I_0 for a given Gaussian intensity distribution of the laser light $I_L = I_0 \exp[-(r/r_0)^2]$. r_0 is the beam radius. I_B/I_0 is calculated according to Eq. (11). We have used the following numbers: $I_0 = 310$ MW/cm^2, $g = 0.02$ cm/MW, $\ell = 50$ cm, $G = 30$.

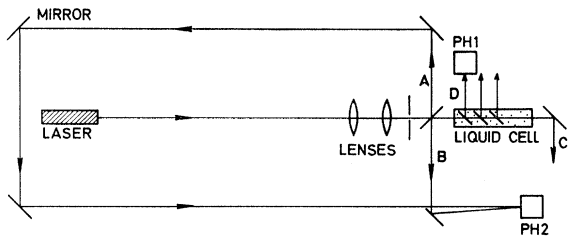

FIG. 2. Experimental setup for the investigation of stimulated Brillouin scattering.

Assuming a Gaussian intensity distribution (13) for the laser light, we integrate $I_B(z)$ over the cross section. The result is

$$\frac{P_B(z)}{P_L(0)} = \frac{G}{I_0 g\ell}\left\{\ln\frac{G}{I_0 g\ell} + \frac{1}{1-\exp(-Gz/\ell)} \times \ln[I_0 g\ell/G + (1 - I_0 g\ell/G)\exp(-Gz/\ell)]\right\}. \quad (15)$$

Equation (15) will be applied directly to the experimental results described in Sec. IV and will be used to determine experimentally the gain factor g.

III. EXPERIMENTAL

In our experiments a ruby laser was used with a maximum (linearly polarized) output power of 1 MW over a diameter of 2 mm, and a beam divergence of 1 mrad. The intensity distribution over the cross section of the output beam was near Gaussian. Fabry-Perot pictures and measurements of the time dependence of the laser pulse with a fast detection system (risetime 0.3 nsec) showed that the laser light was monochromatic with a frequency width smaller than 0.01 cm^{-1}. Oscilloscope pictures revealed consistently the same smooth laser pulse when the laser light was observed through a (movable) pinhole 100 μ in diameter.

The experimental system is depicted in Fig. 2. The distance between the laser and the liquid cell was kept large (400 cm) in order to eliminate multiple Brillouin pulses.[1] The laser intensity was increased by a factor of 9 using an inverted telescope. A small diaphragm (0.5 mm) was used to limit the diameter of the laser beam. The stimulated Brillouin light emitted in the backward direction was coupled out by glass plates outside (B) and inside (D) the liquid cell. The dependence of the Brillouin power on the distance z from the entrance window of the cell was determined as follows. The Brillouin light coming from a glass plate at position z was measured by a fast photocell *Ph*1 and a fast oscilloscope (risetime 0.3 nsec). At the same time the incoming laser power (A) and the Brillouin power (B) leaving the cell (position $z = 0$) were investigated by a second fast detection system (*Ph*2). The laser light was delayed by an optical-delay line and thus could be

measured simultaneously with the Brillouin light in the same detection system (*Ph2*). The transmitted laser light was investigated at position C.

The intensity distribution of the laser and Brillouin light at the entrance window of the cell was investigated by photographing the cell window with a microscope. Fabry-Perot pictures of the Brillouin light were taken at position B.

IV. EXPERIMENTAL RESULTS

A. General Results

We have measured the Brillouin emission and the transmitted laser light in CS_2, *n*-hexane and ethyl ether. The results for *n*-hexane and ethyl ether are very similar. In Fig. 3 measurements on ethyl ether are presented. Oscilloscope traces of the incident laser pulse (A), the back reflected Brillouin pulse (B) and the transmitted laser light (C) are depicted. The Brillouin emission starts with a sharp rise when a definite laser power is exceeded. During the rest of the pulse the Brillouin light follows closely the time dependence of the laser power. The conversion efficiencies are high, they reach maximum values of approximately 75% for *n*-hexane and 80% for ethyl ether. The transmitted light (C) first rises as the incident laser power. At a definite power where noticeable SBS occurs, the transmitted light shows a sharp break. The transmission remains at a low nearly constant level during the rest of the pulse.

The results in CS_2 are somewhat different because in this liquid stimulated Raman scattering is observed in addition to stimulated Brillouin scattering. Figure 4 shows an oscilloscope picture of the total backward emission in CS_2. First a sharp spike occurs which was shown previously[11] to be due to stimulated Raman emission. A detailed discussion of the stimulated Raman emission in CS_2 will be given elsewhere.[12] Almost simultaneously with the Raman spike stimulated Brillouin scattering sets in which continues the rest of the laser pulse with a maximum conversion efficiency of approximately 90%.

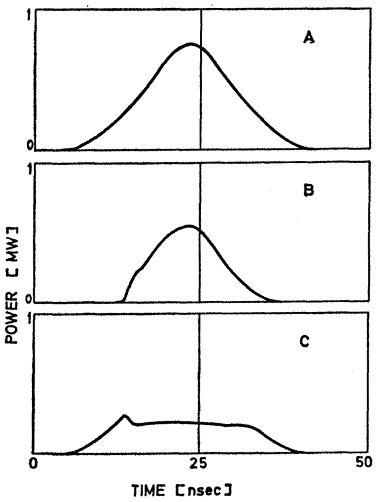

FIG. 3. Oscilloscope traces of the incident laser power (A), the stimulated Brillouin power (B), and the transmitted laser power (C) in ethyl ether.

When beats occurred in the incident laser pulse, the stimulated Brillouin emission (in all three liquids) showed beats with the same frequency. Beat frequencies of 5×10^8 cps were observed occasionally.

Fabry-Perot pictures of the backward emitted light showed frequency shifts which are characteristic for Brillouin scattering of these liquids.[13,14] We found $\Delta\nu=0.193$ cm^{-1} for CS_2, 0.140 cm^{-1} for *n*-hexane and 0.126 cm^{-1} for ethyl ether.

Magnified photographs of the entrance window of the cell indicated that the laser and the Brillouin emission occurred with a nearly Gaussian intensity distribution. The width at the $1/e$ points was $2r_0=0.4$ mm for the laser light and somewhat smaller for the Brillouin light. From the measured maximum laser power of $P_L=1$ MW and the width $r_0=0.2$ mm, a maximum intensity at the center of the beam of approximately $I_0=800$ MW/cm^2 was calculated.

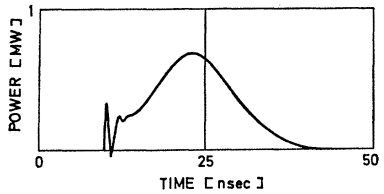

FIG. 4. Oscilloscope trace of the total stimulated emission in the backward direction in CS_2.

B. Quasisteady State

With the experimental system presented in Fig. 2, we were able to make quantitative time resolved measurements of the Brillouin emission. The laser emission was measured simultaneously with the Brillouin emission for each pulse. Representative pictures are shown in Figs. 3 and 4. In Fig. 5 the instantaneous Brillouin power is plotted as a function of the instantaneous laser power for CS_2. The points were obtained from the continuous curves shown in Figs. 3(A), 3(B), and 4 by taking corresponding values of the Brillouin and laser power at different times. Measurements with three different cell lengths are presented. The points (O)

[11] M. Maier, W. Kaiser, and J. A. Giordmaine, Phys. Rev. Letters **17**, 1275 (1966).

[12] M. Maier, W. Kaiser, J. A. Giordmaine, and S. L. Shapiro (to be published).

[13] R. Y. Chiao and P. Fleury, in *Physics of Quantum Electronics*, edited by P. Kelley, B. Lax, and P. Tannenwald (McGraw-Hill Book Co., New York, 1966).

[14] H. Z. Cummins and R. W. Gammon, J. Chem. Phys. 44, 2785 (1966).

correspond to a cell length of 30 cm, (△) and (□) to a length of 5 and 2.5 cm, respectively. The open symbols correspond to values obtained during the rising part of the laser pulse, the full symbols during the decreasing part. After an initial fast rise, a nearly linear dependence of the Brillouin power from the laser power is obtained. For long cells (○) this dependence of the Brillouin power is the same for increasing and decreasing laser power. This observation indicates that the process becomes quasistationary within a short time (≃1 nsec), i.e., a definite laser power creates the same Brillouin power independent of the history of the system. For shorter cells (△) the rapid onset and the quasistationary state are attained at higher laser powers than for long cells. For very short cells (□) a quasistationary state was never reached. Since the process becomes quasistationary in the 30- and 5-cm cell the application of the stationary theory (Sec. II) is justified.

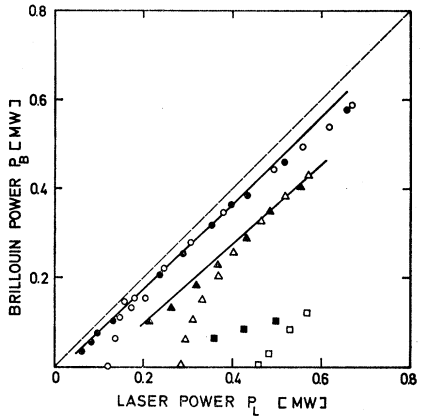

FIG. 5. Instantaneous Brillouin power P_B versus rising (open symbols) and falling (full symbols) instantaneous laser power P_L in CS_2. (○) cell length $\ell=30$ cm; (△) $\ell=5$ cm; (□) $\ell=2.5$ cm. The solid lines are calculated from Eq. (12). The broken line indicates 100% conversion.

The curves in Fig. 5 were calculated from Eq. (12) (see Sec. V, 1). They represent the experimental points remarkably well.

We have measured stimulated Brillouin scattering in *n*-hexane and ethyl ether with cell lengths of 30 and 50 cm. The results are similar to those obtained on CS_2. Again a quasisteady state is found in these liquids as can be seen from Fig. 6 (50-cm cell length of ethyl ether). The calculated curve and the experimental points agree reasonably well.

C. Steady-State Gain Factors

We have determined the dependence of the Brillouin power $P_B(z)$ on the distance z from the entrance window with the experimental setup shown in Fig. 2. Together with the Brillouin power $P_B(z)$ at position z the laser power $P_L(0)$ and the Brillouin power $P_B(0)$ at the entrance window ($z=0$) were measured with fast detection

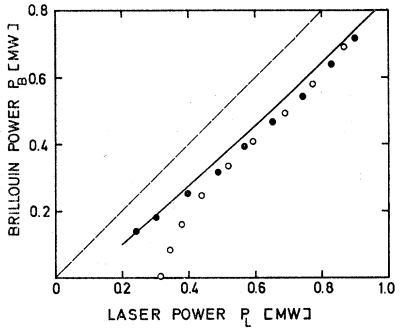

FIG. 6. Instantaneous Brillouin power P_B versus rising (○) and falling (●) instantaneous laser power P_L in a cell of 50-cm length of ethyl ether. The solid line is calculated from Eq. (12). The broken line indicates 100% conversion.

systems. The results of these measurements are shown in Fig. 7. The ratio $P_B(z)/P_L(0)$ taken at the maximum of the laser and Brillouin pulse is plotted as a function of $1/z$ for ethy ether (○) and CS_2 (●). The lines are calculated from Eq. (15) using experimental data for I_0 and ℓ.[15] Values for G and the gain factor g were chosen for the best fit between the calculated curve and the measured points. For CS_2 two curves (B1) and (B2) with different values of G and g are included in Fig. 7 to demonstrate the range of G and g numbers which fit the experimental data. The following numbers were used to calculate the two curves, B1: $g=0.11$ cm/MW, $G=15$, and B2: $g=0.08$ cm/MW, $G=25$. The experimental points are better represented by curve B1 than by B2.

The gain factors g determined in this way (average values obtained from several measurements) are as follows: $g=0.09$ cm/MW ($G=15$) for CS_2 and $g=0.020$ cm/MW ($G=30$) for ethyl ether. For *n*-hexane experimental data similar to those for ethyl ether were obtained and a gain factor of $g=0.016$ cm/MW ($G=30$)

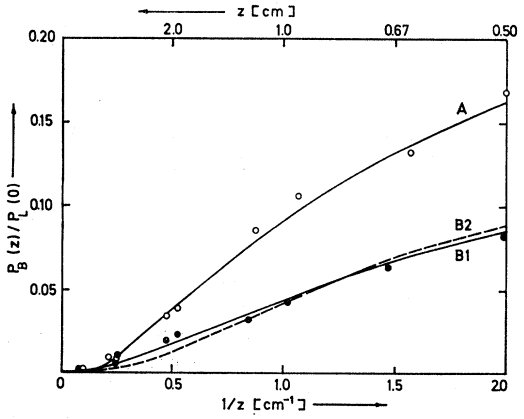

FIG. 7. Measured dependence of the normalized Brillouin power $P_B(z)/P_L(0)$ on the reciprocal distance from the entrance window of the cell $1/z$ (○ ethyl ether, ● CS_2). The lines are calculated from Eq. (15). For further discussion see text.

[15] Experimental data for CS_2: $I_0=500$ MW/cm², $\ell=30$ cm; for ethyl ether: $I_0=800$ MW/cm², $\ell=50$ cm.

was determined. For clarity this curve is omitted in Fig. 7. The accuracy of the experimental g values is approximately $\pm 50\%$. The main sources of error will be discussed in the next section.

It should be noted that most of the conversion of laser light into Brillouin light occurs near the entrance window of the cell. It can be seen from Fig. 7 that the conversion efficiency in CS_2 is $P_B(5\text{ mm})/P_L(0) \simeq 8\%$ at a distance $z=5$ mm. The observed high conversion at the entrance window $P_B(0)/P_L(0) \simeq 90\%$ is created within the first few millimeters of the cell.

V. DISCUSSION

Before discussing the steady-state case a few remarks should be made on the nonstationary behavior of stimulated Brillouin scattering. The experiments of Sec. IV show [see Figs. 3(B) and 4] that stationary SBS is preceded by an initial short nonstationary process. Additional measurements indicated that the nonstationary process becomes dominant for small cell lengths and weak laser intensities. In a previous investigation of SBS Hagenlocker *et al.*[5] obtained agreement between their experimental results and a nonstationary theory[9] in gases and some liquids. A comparison with the results of our paper is difficult because Hagenlocker *et al.* used different substances and different experimental conditions.

As shown in Sec. IV we obtained in our experiments good evidence for a steady-state emission of stimulated Brillouin light. We wish to limit our discussion to this situation. There are three independent experimental observations which will be compared with the steady-state theory outlined in Sec. II.

(1) In the quasisteady state the Brillouin power $P_B(0)$ depends in good approximation linearly on the laser power $P_L(0)$ (see Figs. 5 and 6.) This behavior is expected from Eq. (12), which indicates that to a first approximation $P_B(0)$ is proportional to $P_L(0)$ and smaller than $P_L(0)$ by a nearly constant amount. Using the numbers for g and G determined experimentally in Sec. IV, we have calculated the dependence of the Brillouin power $P_B(0)$ on the laser power $P_L(0)$ according to Eq. (12). The results of the calculations are represented by the full curves in Figs. 5 and 6 which slightly deviate from straight lines. The agreement between the measured and calculated curves is remarkably good for CS_2 and reasonable for ethyl ether. In Table I the measured (Figs. 5 and 6) and calculated [Eq. (12)] maximum power conversion efficiencies for CS_2, ethyl ether and n-hexane are summarized. The good agreement is noteworthy. The dependence of the Brillouin power on the laser power and on the cell length is obviously completely accounted for by the stationary theory [Eq. (12)].

(2) The transmitted laser power $P_L(\ell)$ in n-hexane or ethyl ether is shown in Fig. 3(C). $P_L(\ell)$ is nearly constant in the region of the quasisteady state. A similar behavior was observed in CS_2. The constant transmission of the laser light is explained as follows. Integration of Eq. (8) over the cross section of the beam yields

$$P_L(\ell)=P_L(0)-P_B(0)+P_B(\ell). \tag{16}$$

$P_B(\ell)$ is very small and can be neglected. Using Eq. (12) we obtain

$$P_L(\ell)=(GF_0/g\ell)(1+\ln I_0 g\ell/G). \tag{17}$$

During the quasistationary state the laser power $P_L(0)$ and therefore $I_0=P_L(0)/F_0$ varies less than by a factor of 3. Because of the logarithmic dependence of $P_L(\ell)$ on I_0, $P_L(\ell)$ is approximately constant in agreement with the experimental results.

(3) Now we turn to the discussion of $P_B(z)$, the dependence of the Brillouin power on the distance z from the entrance window. In Sec. IV the experimental data (Fig. 7) were represented by curves calculated according to Eq. (15). The parameters G and g were chosen in such a way to obtain a good fit between the theoretical curve and the experimental points.

It was shown in the previous point (1) that these values of G and g are consistent with the measured dependence of the Brillouin power on the laser power and with the absolute values of the power conversion efficiencies. We now wish to estimate G from classical Brillouin scattering and finally we compare the experimentally determined g values with calculated data.

We first estimate the constant G[Eq. (9)] using classical Brillouin scattering for the determination of the boundary value $I_B(\ell)$. Tang[3,8] has given an expression, which can be used to estimate the Brillouin intensity $I_B(\ell)$ at the end of the cell ($z=\ell$) from classical Brillouin data. Using our experimental data, we evaluate[16] $I_B(\ell)$ for n-hexane, ethyl ether, and CS_2. In all three liquids $I_B(\ell)$ is in the order of magnitude of 10^{-6} W/cm^2. A numerical solution of Eq. (9) for values of $I_L(0)$, g and ℓ in the experimental range of interest gives $G \simeq 30$ for the liquids used. For n-hexane and ethyl ether the

TABLE I. Calculated and measured power conversion efficiencies $P_B(0)/P_L(0)$.

	ℓ[cm]	$P_L(0)$ [MW]	$P_B(0)/P_L(0)$ Calculated	Measured
n-hexane	50	0.9	0.80	0.75
ethyl ether	50	0.9	0.83	0.80
CS_2	30	0.6	0.94	0.90
CS_2	5	0.6	0.75	0.76

[16] According to Eq. (1) of Ref. 3 the Brillouin intensity at the entrance window of the cell is given by $I_B(0)=I_B^{eq}(\ell,\omega_B)\times\Delta\omega_B^{(out)}\times\exp\{I_L(0)g\ell\}=I_B(\ell)\exp\{I_L(0)g\ell\}$. We have assumed that $I_B(\ell)$ is equal to $I_B^{eq}\Delta\omega_B^{(out)}$, with $I_B^{eq}=\Delta\Omega\omega_B^3kT\epsilon/8\pi^3c^2\omega_P$ and $\Delta\omega_B^{(out)}=\alpha_P v_P(\ln 2/I_L(0)g\ell)^{1/2}$. $\Delta\Omega$ is the solid angle subtended by the laser beam ($\Delta\Omega\simeq 10^{-5}$ sr in our experiments), k is the Boltzmann constant, T the temperature, ϵ the dielectric constant, c the velocity of light, and ω_P, α_P, and v_P are the phonon frequency, damping constant, and velocity, respectively (taken from Refs. 4, 13, and 14).

same value $G\simeq 30$ was obtained from the z dependence of $P_B(z)$ (Fig. 7).

In the case of CS_2 the calculated value of $G=30$ is larger than the G value determined from the z dependence ($G=15$–25). This fact suggests that $I_B(\ell)$ in CS_2 is higher than the value calculated from the classical scattering data. This observation may be due to the fact that stimulated Brillouin scattering in CS_2 is initiated by self-focusing action[17] followed by a nonstationary process.[6] Thus, the true initial value for quasistationary SBS may be higher than that calculated from classical Brillouin scattering.

We finally discuss the gain factors g. The values of g determined from the measurements are compared with numbers calculated from Eq. (6). The values of γ and $\gamma^2/n\rho v$[4,13,14] used, and the calculated and measured gain factors g are shown in Table II.

The following remarks should be made concerning the calculation of the g values: The gain factors depend strongly on the literature values of the linewidth $\delta\nu$ and the electrostrictive coupling parameter γ. The $\delta\nu$ values for our calculation are taken from Ref. 4 and 13. Other literature values[18] deviate somewhat from those numbers with an especially large uncertainty for CS_2. This fact might partially account for the difference between calculated and measured g values. The electrostrictive coupling parameter γ is defined as $\gamma=2n\rho(\partial n/\partial\rho)_{ad}=(2n/\beta_{ad})(\partial n/\partial p)_{ad}$. β_{ad} is the adiabatic compressibility, ρ the density and p the pressure. γ was calculated from measurements of $(\partial n/\partial p)_{ad}$ by Raman[19] for CS_2 and ethyl ether. For n-hexane γ was obtained from the formula $\gamma=(n^2-1)\frac{1}{3}(n^2+1)$, which was shown to be a good approximation[19] for the determination of γ.

Concerning the experimental determination of g, the main uncertainties rest in the determination of the absolute values of $P_B(z)$ and especially of I_0.

In summary to point (3) we wish to say that the agreement between the calculated gain factors $g_{\text{calculated}}$ and the measured g_{measured} is considered to be satisfactory taking into account the assumptions made in the theory and the uncertainties in the numbers used.

A quantitative comparison between our gain factors and those obtained from previous investigations is rather difficult, because of the large variations in experimental conditions. The following estimates can be made for n-hexane in spite of this problem: Taking the experimental raw data of Ref. 2 (Fig. 2, curve for laser power 7.5 MW/cm²) and Ref. 3 (Fig. 1, curve for cell length 20 cm) and assuming a steady-state behavior, one calculates steady-state gain factors of approximately 0.045 and 0.024 cm/MW, respectively. It should be noted that Brewer[2] has measured the Brillouin power as a function of cell length and Walder and Tang[3] have investigated the Brillouin emission as a function of laser intensity. Both measurements are made in the region of exponential growth of Brillouin power, while our data ($g=0.016$ cm/MW) were taken in the region of saturation. In view of these differences and the experimental uncertainties the agreement of the gain factors is satisfactory.

TABLE II. Calculated and measured gain factors for stationary stimulated Brillouin scattering.

	$\delta\nu$[MHz]	γ	$\gamma^2/n\rho v$ [cgs units]	$g_{\text{calculated}}$ [cm/MW]	g_{measured} [cm/MW]
n-hexane	222	1.14	1.30×10^{-5}	0.025	0.016
ethyl ether	286	0.94	0.91×10^{-5}	0.014	0.020
CS_2	63	2.3	2.07×10^{-5}	0.14	0.09

VI. CONCLUSIONS

Measurements with high time resolution showed that for n-hexane, ethyl ether, and CS_2 a quasisteady state is reached in stimulated Brillouin scattering if the incoming laser intensity is high enough. For high conversion efficiencies a comparison between experiment and theory was made. The observed linear relationship between Brillouin power and incident laser power, the dependence of the conversion efficiency on the cell length, the approximately constant power transmission, and the dependence of the Brillouin emission on the distance z from the entrance window are well accounted for by a steady-state theory. It was shown that measurements of the z dependence of the Brillouin power are a direct method to determine experimentally the steady state gain factor g of stimulated Brillouin scattering. This method is applicable to any liquid, where a large conversion efficiency and a steady state is observed.

ACKNOWLEDGMENTS

The author is indebted to Professor Dr. W. Kaiser for many helpful suggestions and valuable discussions. He also wishes to thank Dr. K. Grob, D. Pohl, and W. Rother for useful comments during the course of this work.

[17] G. Hauchcorne and G. Mayer, Compt. Rend. **261**, 4014 (1965); Y. R. Shen and Y. J. Shaham, Phys. Rev. Letters **15**, 1008 (1965); P. Lallemand and N. Bloembergen, *ibid.* **15**, 1010 (1965).

[18] A. L. Cederquist, T. Kushida, and L. Rimai (to be published).

[19] C. V. Raman and K. S. Venkataraman, Proc. Roy. Soc. (London) **A171**, 137 (1939).